Pedogeochemistry of ultramafic soils from the Córrego dos Boiadeiros Body, Quadrilátero Ferrífero, Minas Gerais, Brazil

http://dx.doi.org/10.1590/0370-44672017710180

Victor Matheus Tavares Fernandes[1]
http://orcid.org/0000-0001-6347-4922
Hanna Jordt Evangelista[2]
Gláucia Nascimento Queiroga[3]

[1]Mestre em Evolução Crustal e Recursos Naturais, Universidade Federal de Ouro Preto – UFOP, Escola de Minas, Departamento de Geologia, Ouro Preto - Minas Gerais – Brasil.
vmtfernandes@gmail.com

[2]Professora-Titular, Universidade Federal de Ouro Preto – UFOP, Escola de Minas, Departamento de Geologia, Ouro Preto - Minas Gerais – Brasil.
hanna_jordt@yahoo.com.br

[3]Professora-Adjunto, Universidade Federal de Ouro Preto – UFOP, Escola de Minas, Departamento de Geologia, Ouro Preto - Minas Gerais – Brasil.
glauciaqueiroga@yahoo.com.br

Abstract

The Córrego dos Boiadeiros Body (CBB) comprises a metaultramafic-metamafic sequence located in the vicinities of Nova Lima town, central area of the Quadrilátero Ferrífero province. The main rock type is a serpentinite that grades upwards to weathering mantles with well-preserved pedogenetic horizons composed, from bottom to top, of four facies: the R Horizon (Fresh rock facies), the C Horizon (Alterite facies), the B Horizon (Transition facies) and the A Horizon (Solum facies). This article presents the results of geochemical and mass balance studies along a representative pedogenetic profile in order to evaluate the chemical transformations concerning major, trace and Rare Earth Elements. From bottom to top of the selected profile, there is enrichment in Fe_2O_3, Al_2O_3 and depletion in MgO and SiO_2. There are also relative gains of metallic elements as Ni, Co, V and loss of Au. Cr is enriched at the uppermost horizon. Pt is enriched at the basis of the profile, but decreases towards the upper layers. The weathering mantle is REE-enriched and shows major fractionating of LREE over HREE. In order to evaluate the economic potential of the lateritic deposits, especially concerning Cr content, additional chemical analyses should be distributed over the entire body and its surroundings.

Keywords: Quadrilátero Ferrífero; Córrego dos Boiadeiros Body; ultramafic soil; geochemistry; mass balance.

1. Introduction

The Córrego dos Boiadeiros Body (CBB) comprises an association of metaultramafic and metamafic rocks exposed in a 12 km^2 area located near the city of Nova Lima, at the central portion of the Quadrilátero Ferrífero, Minas Gerais State (Figure 1). It is predominantly composed of serpentinite, but steatite, chlorite-tremolite schist, tremolite-serpentine fels and meta-gabbro occur as well. The CBB is a metamafic-metaultramafic sill that belongs to the basis of the Archean Rio das Velhas Greenstone Belt (Costa, 1995). According to Costa (1995), the CBB represents an intrusion in the basal metasedimentary units of the Nova Lima Group.

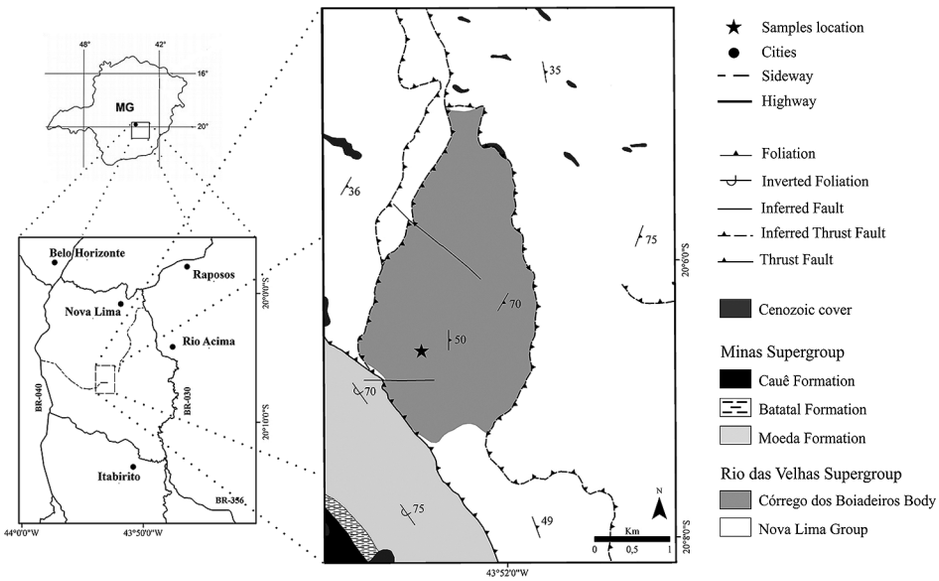

Figure 1
Geographical and geological map of the studied area, modified from Lobato et al., (2005).

The Córrego dos Boiadeiros Body is also characterized by notable weathering mantles developed mainly from the serpentinite and steatite rocks (Figure 2a). Costa (1995) described these weathering mantles as promissory deposits of economic valuable elements, such as Ni, Co, Cr and Platinum Group Elements derived from the metaultramafic source. Reconcentration of these types of elements is very common in soils derived from ultramafic rocks, as described by several authors in many others regions (Elias *et al.*, 1981; Oliveira *et al.*, 1992; Silva and Oliveira, 1995; Cornelius *et al.*, 2008).

This article presents the results of a detailed geochemical investigation and mass balance study of a pedogenetic profile including the fresh rock and the genetically associated weathering mantle. The objective of this study is to understand the formation and the evolution of the ultramafic soils of the CBB and to evaluate its chemical transformations in terms of major, trace and REE (Rare Earth Elements), including those elements with economic value such as Au, Pt, Ni, Co and Cr.

2. Materials and methods

The chosen profile consists of a weathering mantle with well-preserved pedogenetic horizons (Figure 2b). Four samples were collected from drill cores and open pits on the regolith.

Thin sections of the fresh rock were described on a Zeiss Axioscop microscope at the Departamento de Geologia (DEGEO), Universidade Federal de Ouro Preto (UFOP). The composition of the opaque minerals was obtained using a scanning electronic microscope (SEM) JEOL JSM-6010LA with an energy dispersive spectrometer (EDS), at 20 kV, spot size 70, peak counting time 10 s at the Microscopy and Microanalysis Laboratory of DEGEO/UFOP.

The mineralogical characterization of the soil samples was obtained by X-Ray Diffraction (XRD) using an Empyrean Panalytical diffractometer with CuK (α) radiation in an interval of 2° - 70° and step of 0.02° at the X-Ray Diffraction Laboratory of DEGEO/UFOP. The XRD-patterns obtained were processed with the software Origin® 6.0.

Geochemical analyses of major elements were conducted on an Inductively Coupled Plasma Emission Spectrometer (ICP-ES) with sample digestion by HNO_3-acid. Trace and Rare Earth Elements (REE) were analyzed by Inductively Coupled Plasma Mass Spectrometry (ICP-MS) with sample digestion by Aqua Regia (except for metal bases that were molten by Fire Assay). Both analyses were conducted at ACME Analytical Laboratories, Canada.

The density of the fresh rock sample was calculated with a hydrostatic balance at the Environmental Geochemical Laboratory of DEGEO/UFOP, while the density of the soil samples was calculated according to the method of Embrapa (1997). The Embrapa (1997) equation is:

$$Density\ (g/cm^3) = a/b$$

where a – weight of the sample dry at 105°C, b – volume of sample. Also note that b = [(c – d) – e] where: c – weight of paraffined sample, d – weight of sample submerged in water, e – paraffin volume (paraffin weight/0.90).

Mass balance studies were based on the method of Millot and Bonifas (1955). This method, also known as Isovolumetric Calculation, is based on the premise that if an altered soil or saprolite remains with textural and structural characteristics preserved after the alteration process, the variation of volume between the soil and its protolith is null. According to the authors, with the conservation of volume between the fresh rock and the resulting soils, it is possible to calculate the quantity (weight) of each chemical component of a soil or saprolite and compare it with the quantity of the same element in the fresh rock. The Millot and Bonifas (1955) equation is:

$$t\% = 100\,[(da.xa/do.xo) - 1]$$

where t% – element mobility rate, da – density of the alteration product, xa – chemical element content in the alteration product, do – density of the original product, xo – chemical element content in the protolith. The t% value defines the gain (positive) or loss (negative) of the chemical elements in the soils based on its precursor material. The calculations of the mass balance were made using Microsoft Excel spreadsheets.

3. Results

3.1 Petrography and mineralogical characterization

Based on fieldwork, petrography and mineralogical characterization, four facies were defined in this study. They are defined, from the bottom to the top of the profile, as the R Horizon (Fresh rock facies), the C Horizon (Alterite facies), the B Horizon (Transition facies) and the A Horizon (Solum facies). The nomenclature cited in parenthesis was adopted according to Lacerda *et al.*, (2002).

The Fresh rock facies is an olive green serpentinite with inequigranular fine- to medium-grained texture and a well-developed foliation. Subordinate veins composed of carbonate, talc or serpentine cross-cut the rock (Figure 2c). The serpentinite shows decussate microstructure (Figure 2d), although small amount of lepidoblastic serpentine lamellae is also found. The fresh serpentinite is composed of serpentine (90 to 95 vol%) and opaque minerals (5 to 10%) identified by SEM/EDS analyses as magnetite, chromite and rare pyrrhotite and pentlandite.

Figure 2
a) Ultramafic weathering mantle (brown color) on top of the serpentinite body at the Pedras Congonhas mine. b) Weathering mantle showing the studied pedogenetic horizons. c) Drill core with the Fresh-rock facies (serpentinite with white carbonate veins). d) Photomicrograph of serpentinite, with serpentine (Srp) lamellae and magnetite (Mag) grains (XPL). XPL: crossed polarized light.

The Alterite facies is comprised of gray to brownish saprolite. This horizon usually ranges from 60 to 70 cm of thickness and occurs in a transitional contact with the underlying horizon (Fresh rock facies). The Alterite facies commonly preserves the protolith foliation (original rock feature) being composed of massive pieces of fresh rock, which macroscopically displays remnants of serpentinite surrounded by weathered materials. There are slightly altered veins of antigorite (serpentine) or talc whereas ferruginous nodules are absent. The XRD-pattern of the Alterite facies indicates the presence of minerals from the protolith as talc, magnetite, antigorite and chromite (Figure 3).

The Transition facies has an average thickness of 120 cm and is characterized by a light-brown horizon situated above the Alterite facies. The contact is transitional with the underlying horizon (Alterite facies), marked by the first appearance of tiny ferruginous nodules, which are absent in the underlying horizons, and by the disappearance of relict textures of the protolith. The X-ray diffraction pattern shows that it differs from the underlying horizon by the absence of magnetite and the presence of kaolinite, gibbsite and goethite (Figure 3).

The uppermost layer of the weathering mantle corresponds to the Solum facies. This horizon occurs in an abrupt contact with the underlying Transition facies displaying an average thickness of 90 cm. It is composed of brown to reddish soil which exhibits a large scale of coarse-grained ferruginous nodules, which range from 2 cm to 5 cm in diameter. Lastly, the Solum facies is characterized by the complete disappearance of most minerals derived from the protolith as talc, magnetite and antigorite. It is mostly composed of hydroxides such as goethite and gibbsite, as well as chromite and kaolinite (Figure 3).

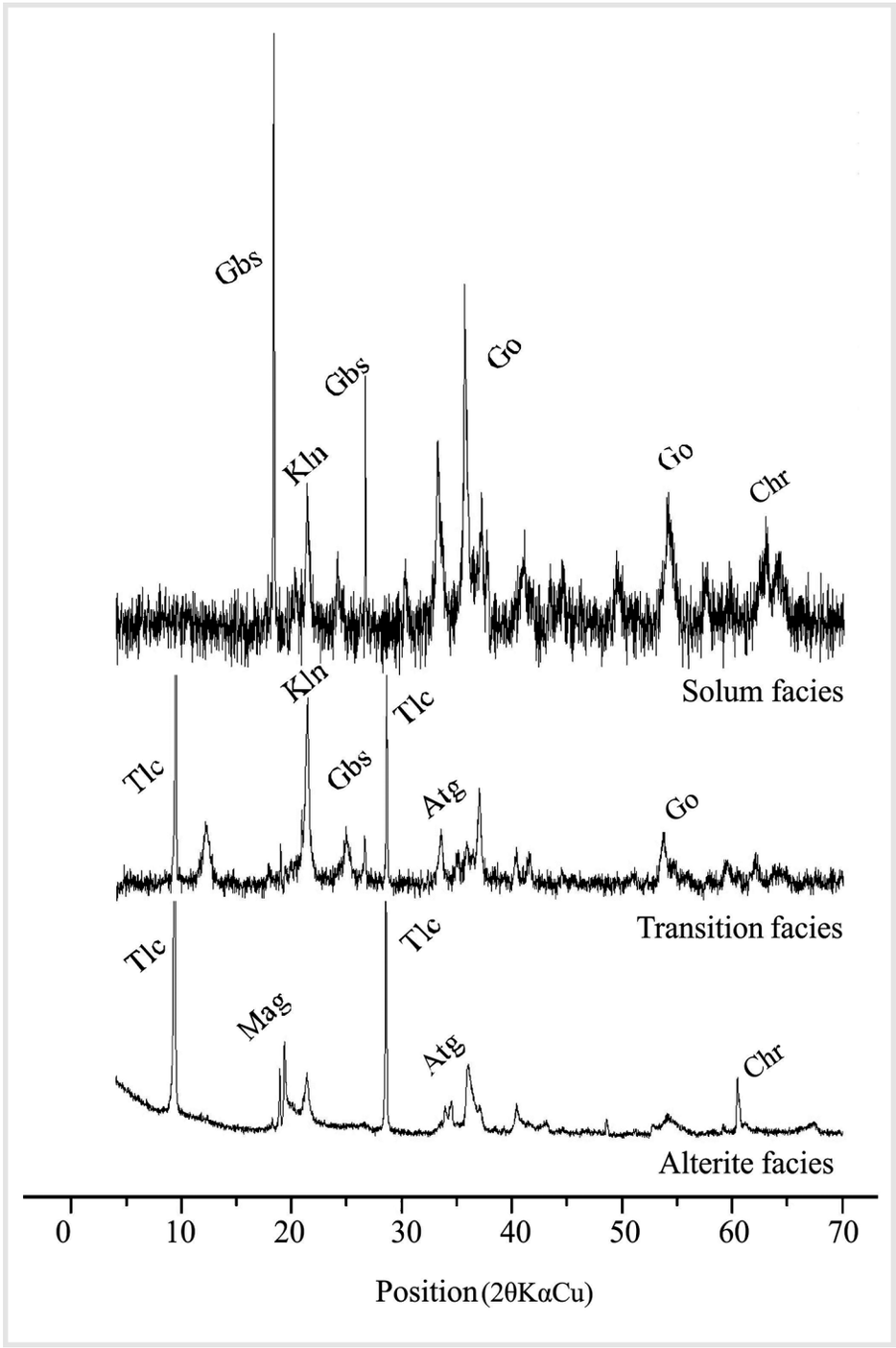

Figure 3
X-ray diffraction patterns (CuKα radiation) of Alterite, Transition and Solum facies. Atg: Antigorite, Chr: Chromite, Gbs: Gibbsite, Go: Goethite, Kln: Kaolinite, Mag: Magnetite, Tlc: Talc.

3.2 Geochemistry

In comparison to the other facies, the Fresh rock facies has higher concentrations of MgO (33.02 wt%) and CaO (0.18%), and lower concentrations of TiO_2 (0.08%), Al_2O_3 (2.07%), Fe_2O_3 (5.44%) and Cr_2O_3 (0.45%) (Table 1). It also shows considerable amounts of Ni (529 ppm), Au (9 ppb) and the lowest contents of Co (89.5 ppm), V (70 ppm) and REE if compared with the other horizons of this study. The density of the sample is 2.80 g/cm³.

	R Horizon (Fresh rock facies)	C Horizon (Alterite facies)	B Horizon (Transition facies)	A Horizon (Solum facies)	Detection Limit
SiO_2	45.76	53.03	21.77	3.81	0.01
TiO_2	0.08	0.17	0.66	0.40	0.01
Al_2O_3	2.07	5.15	16.08	20.47	0.01
Fe_2O_3*	5.44	11.23	42.89	52.96	0.04
MnO	0.16	0.16	0.79	0.61	0.01
MgO	33.02	21.59	3.35	0.28	0.01
CaO	0.18	0.02	0.05	0.01	0.01
Na_2O	0.01	<0.01	<0.01	<0.01	0.01
K_2O	<0.01	<0.01	0.08	<0.01	0.01
P_2O_5	<0.01	<0.01	<0.01	<0.01	0.01
Cr_2O_3	0.45	0.62	0.68	3.84	0.002
LOI**	12.2	7.5	13.2	17.0	-
Total	99.43	99.59	99.71	99.72	-
Ni	529	1000	949	2630	20
Co	89.5	156.9	924.9	942.3	0,2
V	70	140	256	309	8
Au***	9	4	10	3	2
Pt***	4	11	12	4	3
La	0.7	1.3	13.7	8.6	0.1
Ce	0.6	2.0	10.8	12.6	0.1
Pr	0.08	0.36	3.66	2.60	0.02
Nd	0.4	1.7	14.9	11,5	0.3
Sm	0.08	0.37	2.73	2.77	0.05
Eu	0.04	0.09	1.09	0.65	0.02
Gd	0.16	0.47	2.45	2.36	0.05
Tb	0.03	0.09	0.43	0.42	0.01
Dy	0.24	0.74	2.69	2.41	0.05
Ho	0.05	0.16	0.57	0.54	0.02
Er	0.15	0.60	1.88	1.73	0.03
Tm	0.02	0.09	0.34	0.27	0.01
Yb	0.18	0.71	2.25	2.01	0.05
Lu	0.03	0.11	0.37	0.32	0.01
∑REE	2.76	8.79	57.86	48.78	-
Density (g/cm³)	2.80	2.11	1.64	1.76	-

* All Fe as Fe_2O_3; ** Loss of ignition; *** values in ppb

Table 1
Chemical composition of major (wt%), trace (ppm) and Rare Earth Elements (ppm) and densities of the reference lithotype (R horizon) and the pedogenetic horizons.

The Alterite facies has the highest amount of SiO_2 (53.03 wt%). It also shows intermediate values of major and trace elements. In terms of REE, the horizon has higher contents than the protolith, but shows much fewer amounts than the Transition and Solum facies (Table 1). It also shows the lowest LOI (7.5%) of the analyzed samples. The density is 2.11 g/cm³.

The Transition facies shows the highest concentrations of TiO_2 (0.66 wt%), MnO (0.79%), Pt (12 ppb) and Au (10 ppb). It is the only facies with contents of K_2O above the detection limit (0.08%). The Transition facies has the highest LREE (Light Rare Earth Elements) concentrations as La (13.7 ppm), Pr (3.66 ppm) and Nd (14.9 ppm). It also has the highest REE concentration in general (sum 57.86 ppm). The density is 1.64 g/cm³ (Table 1).

The Solum facies is characterized by the lowest contents of SiO_2 (3.81 wt%), MgO (0.28%), CaO (0.01%), Au (3 ppb) and Pt (4 ppb). This horizon is the most enriched in Al_2O_3 (20.47%), Fe_2O_3 (52.96%), Cr_2O_3 (3.845%), Ni (2630 ppm), Co (942.3 ppm) and V (309 ppm). In terms of Rare Earth Elements, the Solum Facies has the highest Ce concentration (12.6 ppm) whereas HREE (Heavy Rare Earth Elements) contents are very similar to the Transition facies. The density is 1.76 g/cm³ (Table 1).

3.3 Mass balance

Normalized by the chemical composition of the protolith (R horizon), the behavior of major elements in the weathering mantle indicates a progressive enrichment of Al_2O_3 and Fe_2O_3 from the bottom to the top. It also shows a decrease of SiO_2, MgO and CaO. There are losses of MnO in the Alterite facies, but gains of this oxide in the Transition and Solum facies. TiO_2 shows expressive gains in the Alterite and Transition facies, but a relative loss in the Solum facies. Cr_2O_3 remains slightly constant in the C and B horizons and shows enrichment in the uppermost horizon (Figure 4).

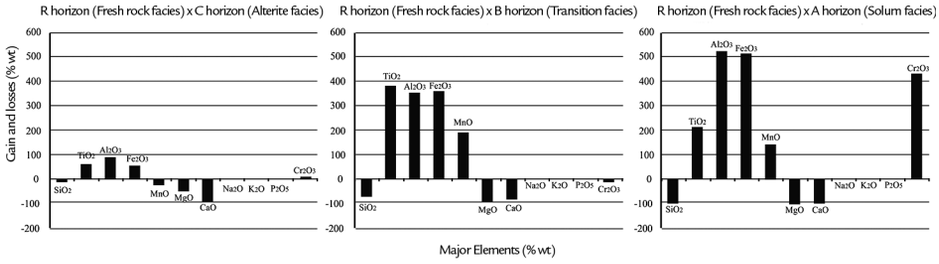

Figure 4
Chemical distribution of the major elements in the pedogenetic horizons of the weathering mantle, normalized by the Fresh rock facies chemical composition.

The behavior of the trace elements indicates a gain of V in all horizons of the weathering mantle. Ni is enriched in the Solum facies and Co shows an exponential enrichment from the Alterite to the Transition and Solum facies. Au is depleted in all horizons of the weathering mantle. Pt is highly enriched in the Alterite facies but shows progressive losses in the upper facies (Figure 5).

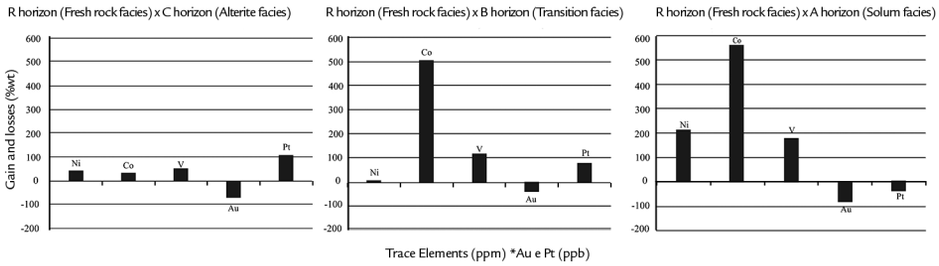

Figure 5
Chemical distribution of trace elements in the pedogenetic horizons of the weathering mantle, normalized by the Fresh rock facies chemical composition.

Based on the chemical composition of the protolith (R horizon), the behavior of REE indicates a progressive enrichment towards the top of the weathering mantle. There is observed a discreet gain of all REE in the Alterite facies, followed by exponential gains in the Transition and Solum facies (Figure 6). By using the mass balance, there is also observed a higher concentration of LREE than HREE in the upper horizons of the weathering mantle.

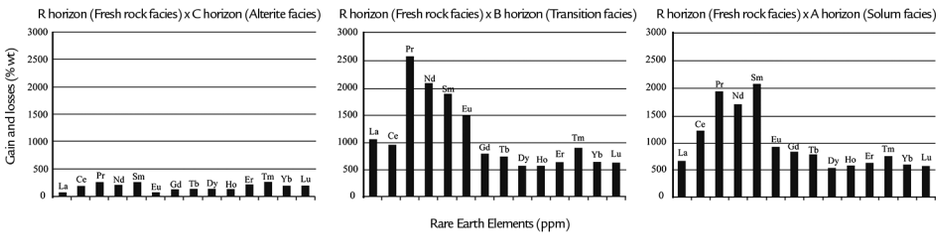

Figure 6
Chemical distribution of the Rare Earth Elements in the pedogenetic horizons of the weathering mantle, normalized by the Fresh rock facies chemical composition.

4. Discussion

In terms of the major elements, the chemical evolution of the weathering mantle indicates a progressive enrichment of Fe_2O_3, Al_2O_3 and a decrease of MgO, CaO and SiO_2 from bottom to top in the selected profile. This behavior is a result of the weathering increase that hydrolyzes primary and clay minerals, leaching preferentially Mg, Ca and Si from the system and reveals less mobility elements like Fe and Al that concentrate in the residual soil profile (Trescases, 1975). According to Silva and Oliveira (1995) this represents the most typical evolution of the ultramafic soils. In this study, the X-ray diffraction patterns show the presence of Fe and Al hydroxides, like goethite and gibbsite and the absence of Mg and Si minerals as serpentine (antigorite) and talc in the upper horizons, corroborating the observed chemical evolution. Although Ti is an immobile element during weathering conditions, remaining stable on the soil profile, it is being proportionally enriched in response to the concentration decreasing of mobile elements like Mg, Ca and Si (Cramer and Nesbit, 1983).

The peculiar chromium behavior that increases about 400% from the fresh rock to the top of the profile is similar to that described for serpentinite soils by Hotz (1964), Rabenhorst *et al.*, (1982) and Gough *et al.*, (1989). According to the observations of these authors, the concentration of Cr_2O_3 in weathering mantles typically increases from the bottom to the top of the profile. Furthermore, Oze *et al.*, (2004) suggest that the accumulation of Cr_2O_3 in ultramafic soils depends exclusively on the presence of the weathering resistant phases, such as chromite. The XRD-pattern (Figure 3) shows the presence of chromite in the Solum facies, which is the highest Cr_2O_3-enriched horizon.

Nickel is enriched almost 200% in the weathering mantle. Oliveira *et al.*, (1992) suggest that this accumulation may

be related to the Ni concentration in goethite during the weathering of the ultramafic source under oxidizing conditions. Vanadium gains in ultramafic weathering mantles are described by Kabata-Pendias (2011) as the result of incorporation of this element in the structure of hydrous ferric oxides. Cobalt exhibits enrichment along all the profile, culminating with gains around 500%. According to McKenzie (1972), this behavior is associated with the sorption of Co or the partial substitution of Mn by Co in Mn-Fe oxides

Platinum exhibits a relatively high concentration in the lower portion of the weathering mantle and depletion in the upper part of the profile. This pattern is also noticed by Traoré *et al.,* (2008) and Ndjigui and Bilong (2010) in other ultramafic soils. The concentration of Pt at the bottom of the profile occurs in response to the precipitation of PGE alloys with iron oxides (Bowles, 1986; Bowles *et al.,* 1994; Wimpenny *et al.,* 2007). There is no consensus among these authors about the cause of the depletion of Pt in the uppermost layer, but is probable that the natural processes of pedogenesis may solubilize and remobilize this element under oxidizing conditions.

The chondrite-normalized REE patterns shows a great enrichment of LREE over HREE in the weathering mantle (Figure 7). Alterite facies show that the gains of LREE are slightly superior to the gains of HREE. Furthermore, Transition and Solum facies have similar patterns characterized by the high enrichment of LREE over HREE, with emphasis to the gains of La, Pr and Nd. This fractionation pattern is also described by Braun *et al.,* (1998) in lateritic soils. The total REE content (ΣREE) shows enrichment from 2.76 ppm in the protolith to 48.78 ppm in the Solum facies (Table 1). This enrichment indicates that the REE remained relatively mobile during the pedogenetic process.

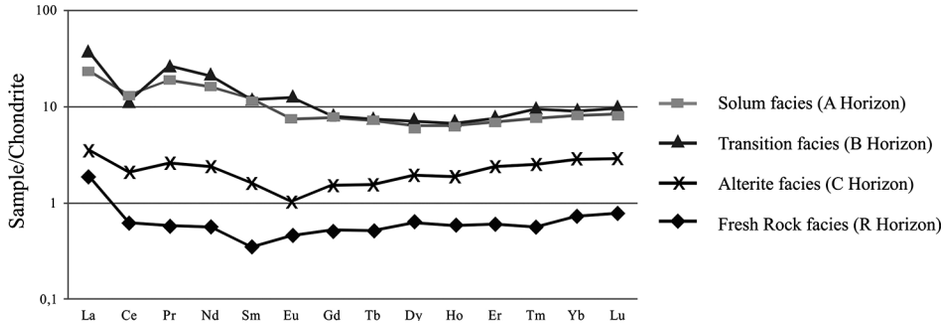

Figure 7
Chondrite-normalized REE patterns of the weathering mantle and its protolith; normalizing values from Evensen et al., (1978).

5. Conclusions

The studied weathering mantle was generated under oxidizing conditions through processes of pedogenesis on serpentinite as the parental material. Geochemical and mass balance investigations along the soil profile allowed the identification of chemical distribution patterns of the selected elements. From bottom to top, there is enrichment in Fe_2O_3 and Al_2O_3 and depletion of MgO and SiO_2. The enrichment of Fe_2O_3 is related to the ferruginous nodules, observed on the top of the soil profile whereas Al_2O_3 is related to gibbsite accumulations. The soil profile exhibits a gain on metallic elements as Ni, Co, V and loss of Au. Cr shows enrichment in the upper horizons. Pt is enriched at the bottom of the profile, and depleted in the uppermost layers. The REE present major fractionating of LREE over HREE and are largely enriched in the weathering mantle, as a result of the relatively mobile behavior of these elements during pedogenesis. In order to accurately investigate the economic viability of metallic elements related to the local lateritic deposits, it is advisable to increase the number of chemical analyses in the CBB weathering mantle and surrounding areas.

Acknowledgements

The first author thanks CAPES for the master scholarship. The authors thank Pedras Congonhas Extração Arte e Indústria Ltd. for financial and logistic support. We are also grateful to the Microscopy and Microanalysis Laboratory (LMIc) of the Universidade Federal de Ouro Preto, a member of the Microscopy and Microanalysis Network of Minas Gerais State/Brazil/FAPEMIG, for the mineral chemistry analyses. G. Queiroga is fellow of the Brazilian Research Council (CNPq) and acknowledge for the support received.

References

BOWLES, J. F. W. The development of platinum-group minerals in laterites. ***Economic Geology,*** v. 81, p. 1278-1285, 1986.

BOWLES, J. F. W., GIZE, A. P., COWDEN, A. The mobility of the platinum-group elements in the soils of the Freetown Peninsula, Sierra-Leone. ***Canadian Mineralogist,*** v. 32, p. 957-967, 1994.

BRAUN, J. J., VIERS, J., DUPRÉ, B., POLVE, M., NDAM, J., MULLER, J. P. Solid/liquid REE fractionation in the lateritic system of Goyoum, East Cameroon: the implication for the present dynamics of the soil covers of the humid tropical regions. ***Geochimica et Cosmochimica Acta,*** v. 62, n. 2, p. 273-299, 1998.

COSTA, C. S. ***Petrogênese do corpo metaultramáfico do córrego dos Boiadeiros,***

Quadrilátero Ferrífero, Minas Gerais, Brasil. Belo Horizonte: Universidade Federal de Minas Gerais, Instituto de Geociências, 1995. 172 p. (Dissertação de mestrado).

CORNELIUS, M., ROBERTSON, I. D. M., CORNELIUS, A. J., MORRIS, P. A. Geochemical mapping of the deeply weathered western Yilgarn Craton of Western Australia, using laterite geochemistry. ***Geochemistry: Exploration, Environment, Analysis,*** v. 8, p. 241-254, 2008.

CRAMER, J. J., NESBIT, H. J. Mass-balance relations and trace-element mobility during continental weathering of various igneous rocks. ***Science and Géology Mémoires,*** v. 73, p. 63-73, 1983.

ELIAS, M., DONALDSON, M. J., GIORGETTA, N. E. Geology, mineralogy, and chemistry of lateritic nickel-cobalt deposits near Kalgoorlie, Western Australia. ***Economic Geology,*** v. 76, p. 1775-1783, 1981.

EMBRAPA. Serviço Nacional de Pesquisa dos Solos (Rio de Janeiro, RJ). Manual de métodos de análise do solo. (2 ed.). Rio de Janeiro, 1997. 212p.

EVENSEN, N. M., HAMILTON, P. J., O'NIONS, R. K. Rare earth abundances in chondritic meteorites. ***Geochimica et Cosmochimica Acta,*** v. 42, p. 1199-1212, 1978.

GOUGH, L. P., MEADOWS, G. R., JACKSON, L. L., DUDKA, S. Biogeochemistry of a highly serpentinized, chromite-rich ultramafic area, Tehama County, California. U.S. ***Geological Survey Bulletin,*** v. 1901, p. 1-24, 1989.

HOTZ, P. E. Nickeliferous laterites in southwestern Oregon and northwestern California. ***Economic Geology,*** v. 59, p. 355-396, 1964.

KABATA-PENDIAS, A. ***Trace elements in soils and plants.*** Boca Raton, Florida: CRC Press, 2011. 505p.

LACERDA, M. P. C., ANDRADE, H., QUÉMÉNEUR, J. J. G. Pedogeoquímica em perfis de alteração na região de Lavras (MG). II – Elementos menores e elementos das terras raras. ***Revista Brasileira de Ciência do Solo,*** v. 26, p. 87-102, 2002.

LOBATO, L. M., BALTAZAR, O. F., REIS, L. B., ACHTSCHIN, A. B., BAARS, F. J., TIMBÓ, M. A., BERNI, G. V., MENDONÇA, B. R. V., FERREIRA, D. V. Projeto Geologia do Quadrilátero Ferrífero – integração e correção cartográfica em SIG com nota explicativa. Belo Horizonte: CODEMIG, 2005. 1 CD-ROM.

MCKENZIE, R. M. The sorption of some heavy metals by the lower oxides of manganese. ***Geoderma,*** v. 8, p. 29-35, 1972.

MILLOT, G., BONIFAS, M. Transformations isovolumetriques dans les phenomenes de laterisation et de bauxitisation. ***Bulletin Service Carte Géolique Alsace et Lorraine,*** v. 8, p. 3-10, 1955.

NDJIGUI, P. D., BILONG, P. Platinum-group elements in the serpentinite lateritic mantles of the Kongo-Nkamoua ultramafic massif (Lomié region, South-east Cameroon). ***Journal of Geochemical Exploration,*** v. 107, p. 63-76, 2010.

OLIVEIRA, S. M. B., TRESCASES, J. J., MELFI, A. J. Lateritic nickel deposits of Brazil. ***Mineralium deposita,*** v. 27, p. 137-146, 1992.

OZE, C., FENDORF, S., BIRD, D. K., COLEMAN, R. G. Chromium geochemistry of serpentinite soils. ***International Geology Review,*** v. 46, p. 97-126, 2004.

RABENHORST, M. C., FOSS, J. E., FANNING, D. S. Genesis of Maryland soils formed from serpentinite. ***Soil Science Society of America Journal,*** v. 46, p. 607-616, 1982.

SILVA, M. L. M. C., OLIVEIRA, S. M. B. As fases portadoras de níquel do minério laterítico de níquel do vermelho, Serra dos Carajás (PA). ***Revista Brasileira de Geociências,*** v. 25, n. 1, p. 69-78, 1995.

TRAORÉ, D., BEAUVAIS, A., AUGÉ, T., PARISOT, J. C., COLIN, F., CATHELINEAU, M. Chemical and physical transfers in an ultramafic rock weathering profile: Part 2. Dissolution vs. accumulation of platinum group minerals. ***American Mineralogist,*** v. 93, p.31-38, 2008.

TRESCASES, J. J. ***L'évolution géochimique supergène des roches ultrabasiques em zone tropicale - formation des gisements nickélifères de Nouvelle-Calédonie. Mémoires de ORSTOM,*** 1975. 259 p.

WIMPENNY, J., GANNOUN, A., BURTON, K. W., WIDDOWSON, M., JAMES, R. H., GÍSLASON, S. R. Rhenium and osmium isotope and elemental behavior accompanying laterite formation in the Deccan region of India. ***Earth and Planetary Science Letter,*** v. 261, p. 239-258, 2007.

Received: 7 December 2017 - Accepted: 3 June 2018.